Modelling and Control of the Dual Smart Drive

Roemi Fernández, Teodor Akinfiev, Manuel Armada

Abstract— **This paper summarizes ongoing work with the dual drive, a special drive with continuously changing transmission ratio and dual properties, intended for usage in walking machines and other kind of robotic systems in which the same drive is used to perform two essentially different types of start-stop motions of the executive link. The description of the latest version of the drive, its dynamic model and the developed control algorithm are some of the main topics discussed here. Results of experimental trials are also presented in order to evaluate the system performance.**

Keywords— **Dual smart drive, quasi-resonance drive, start-stop regime, non-linear transmission ratio, harmonic linearization, adaptive control, walking robots.**

I. Introduction

THE walking process in legged robots is composed of two different phases. The first one is the swing phase when one or more legs are on the ground while the other swings. The second phase takes place when all the legs are on the ground while the body is moving forward. Consequently, in walking robots, the drive of a leg works in two rather different regimes. First, the drive is utilized for the movement of the leg in relation to the fixed body. After that, the same drive is employed for the movement of the heavy body of the robot in relation to the fixed leg. The low performance of conventional drives (electrical motor with constant reduction gear) when moving in start-stop regime is well known. Earlier studies [1-3] have demonstrated that the use of resonance and quasi-resonance drives instead of conventional ones allows a significant increasing in both the machine velocity and the effectiveness of drive motor. In this way, the use of the SMART drive [4] in a biped locomotion proved to reduce the energy consumption up to 75%. Nevertheless, this condition, which is typical in resonance and quasi-resonance drives, is only true when the system is set up with an appropriate tuning. Hence, the drive adjusted on one of the regimes in optimal mode, appears to be inefficient in the second one. To solve the problem arising from the necessity of using the same drive to produce two different types of motions in walking robots, a new drive, called DUAL SMART drive [5], has been designed in the Industrial Automation Institute.

Roemi Fernández is with the Industrial Automation Institute, Spanish Council for Scientific Research, Automatic Control Department, La Poveda - Arganda del Rey, Madrid 28500, Spain. E-mail: roemi@iai.csic.es.

Teodor Akinfiev was with Mechanical Engineering Research Institute of Russian Academy of Sciences, Russia, Moscow. He is now with the Industrial Automation Institute, Spanish Council for Scientific Research, Automatic Control Department, La Poveda - Arganda del Rey, Madrid 28500, Spain.

Manuel Armada is with the Industrial Automation Institute, Spanish Council for Scientific Research and he is the head of the Automatic Control Department, La Poveda - Arganda del Rey, Madrid 28500, Spain.

Bearing these facts in mind, the paper is organized as follows. Section two describes the DUAL SMART drive system configuration. Section three formulates its dynamic model and derives an approximate analytical solution with the aim of demonstrating the behavior response of the system. Section four presents the control algorithm. Section five shows the results of experimental tests prepared with the manufactured prototype. Finally, section six presents the main conclusions and directions toward future developments.

II. The Dual Smart Drive

The configuration of the DUAL SMART drive is presented on figure 1. A DC motor fixed on the body of the robot is connected with a reducer, which has a constant gear ratio K_G. The kinematic connection between the reducing gear and the leg of the robot contains a link (fixed on the body with a possibility of rotation), a slider (arranged on the link), and a crank connected with the reducing gear. The slider is fixed on the link with the possibility of slipping along it in a radial direction. The crank is hinged with the slider by means of a finger. The link is connected kinematically to the leg of the robot (this kinematic connection can be carried out as an additional reducing gear, gear wheel - rod transmission, etc.; in the simplest case this kinematic connection can be implemented with the help of immediate usage of a link as a leg of the robot). The motor is also linked to the control system, which has corresponding sensors.

For this system, the kinematics is determined by the following parameters (see figure 2): L - distance between the link rotation axis and the crank rotation axis, R - length of the crank $[R < L]$, α - angular position of the crank, measured clockwise from the ox axis, β - angular position of the mobile link, measured clockwise from the ox axis. Figure 3 shows that the link will move between two extreme positions:

$$-\beta_0 < \beta < \beta_0 \tag{1}$$

where β_0 is defined as:

$$\beta_0 = \arcsin\left(\frac{R}{L}\right) \tag{2}$$

A displacement of the link from one extreme position to the other one can be carried out in two ways - by displacement of the crank within the limits of the angle γ_1 or within the limits of the angle γ_2. The variation of β in function of α is given by:

$$\beta = arctg\left(\frac{Sin\alpha}{(L/R) + Cos\alpha}\right) \tag{3}$$

According to definition, the transmission ratio between the reducing gear and the link can be calculated as follows:

$$K_D = \frac{\dot{\alpha}}{\dot{\beta}} \Rightarrow K_D = \frac{1 + (L/R)^2 + 2(L/R)Cos\alpha}{1 + (L/R)Cos\alpha} \quad (4)$$

where $\dot{\alpha}$ is the angular velocity on the reduction gear shaft and $\dot{\beta}$ is the angular velocity of the mobile link.

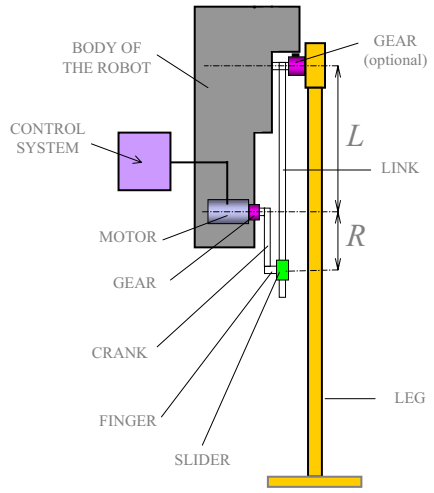

Fig. 1. Configuration of the Dual Smart Drive

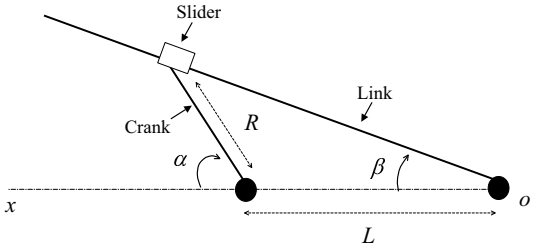

Fig. 2. Kinematical schema of the drive

The figure 4 shows that this relationship has a 2π periodic character consisting in two different parts: one part with negative values (part γ_2), and another part with positive values (part γ_1). The negative magnitude of the reduction ratio means that the crank and the link are rotating in opposite directions. It is interesting that the reduction ratio tends to infinity in the extreme points, $-\beta_0$, and β_0, where the crank is perpendicular to the link. In these points, the deviation of the link from its medium position is maximal. Accordingly, in the same points, the deviation of robot's leg (kinematically connected with the link by a transmission with a constant value of the reduction ratio) from its medium position is maximal, too. That is why, the movement from one extreme position to another ensures the most favorable change of the reduction ratio for maintaining high accelerations of a working element in the beginning and in the end of driving (high absolute magnitude of the reduction ratio) and for maintaining high speeds in an intermediate part of the trajectory (low absolute magnitude of the reduction ratio).

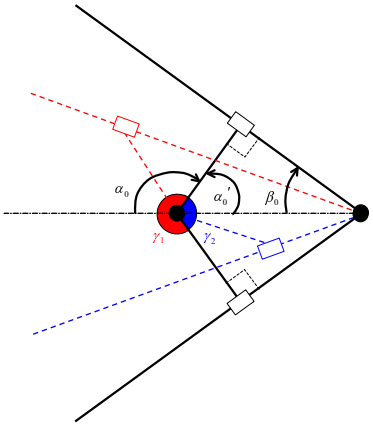

Fig. 3. Kinematical schema of the drive

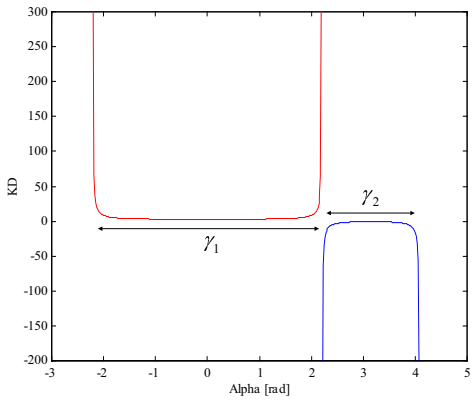

Fig. 4. Transmission ratio K_D vs. angular position of the crank

Thus, the changeover can be carried out both within the limits of the angle γ_1 and within the limits of the angle γ_2. At displacement within the limits of the angle γ_1 the absolute average magnitude of the reduction ratio will be greater, than at displacement within the limits of the angle γ_2. This enables to use the movements of the crank within the limits of one angle, when the loading is small (and to gain high speeds of displacement), or within the limits of the other angle, when the drive loading is great (having, correspondingly, smaller velocities of displacement). Figure 5 shows the difference between the two absolute magnitudes of the reduction ratios as function of β. Therefore, the drive allows easily to realize a displacement of the working element from one extreme position to another and to have two different laws of change

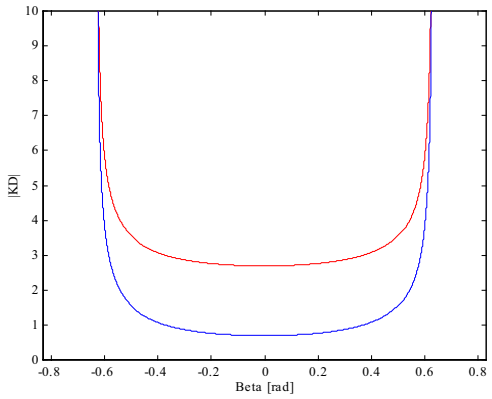

Fig. 5. Absolute magnitudes of the transmission ratios K_{D1} and K_{D2} vs. β

of a drive reduction ratio.

III. Model for The Dual Smart Drive

Assuming a horizontal movement, the dynamic model of the system with a non-linear transmission ratio can be expressed by:

$$J_{eqi}\ddot{\beta} = M_{\beta i} - b_{eqi}\dot{\beta} - M_{FRi}sign\left(\dot{\beta}\right), \tag{5}$$

where J_{eqi} is the equivalent inertia of the mobile element on each working regime $i = [1-2]$, $\ddot{\beta}$ is the angular acceleration of the mobile element, $M_{\beta i}$ is the equivalent moment of the motor on the mobile element, b_{eqi} is the equivalent viscosity friction coefficient and M_{FRi} is the moment of friction on each regime. The equivalent moment of the motor on the mobile element is given by:

$$M_{\beta i} = K_{Di}K_G M_{Mi}, \tag{6}$$

where K_{Di} is the DUAL SMART transmission, K_G is the constant reduction gear ratio and M_{Mi} is the moment of the motor. The DUAL SMART transmission ratio on each regime is given by:

$$K_{D1} = \frac{1 + (L/R)^2 + 2(L/R)k_1'}{1 + (L/R)k_1'} \tag{7}$$

$$K_{D2} = \frac{1 + (L/R)^2 - 2(L/R)k_2'}{1 - (L/R)k_2'}, \tag{8}$$

where

$$k_1' = Cos\left(\beta + arcSin[(L/R)Sin(\beta)]\right)$$

$$k_2' = Cos\left(\beta - arcSin[(L/R)Sin(\beta)]\right)$$

The moment of the motor has the form:

$$M_{Mi} = k_m I_i, \tag{9}$$

where k_m is the torque constant and I_i is the armature current. The armature current I_i is given by:

$$I_i = \frac{U_i}{R_M} - \frac{k_E}{R_M}\dot{\varphi}_i, \tag{10}$$

where U_i is the motor terminal voltage, R_M is the armature resistance, k_E is the back - EMF constant and $\dot{\varphi}_i$ is the angular velocity of the motor. The varying motor terminal voltage is described by the equations:

$$U_1 = \zeta\left(\dot{\beta}\right)\left[U_{01}\zeta\left(-\beta\right) + U_{F1}\zeta\left(\beta\right)\right] - \\ - \zeta\left(-\dot{\beta}\right)\left[U_{01}\zeta\left(\beta\right) + U_{F1}\zeta\left(-\beta\right)\right], \tag{11}$$

$$U_2 = \zeta\left(\dot{\beta}\right)\left[U_{02}\zeta\left(\beta\right) + U_{F2}\zeta\left(-\beta\right)\right] - \\ - \zeta\left(-\dot{\beta}\right)\left[U_{02}\zeta\left(-\beta\right) + U_{F2}\zeta\left(\beta\right)\right], \tag{12}$$

where ζ is the Heaviside function and U_{01}, U_{02}, U_{F1} and U_{F2} are constant values of voltage. Finally, the angular velocity of motor as function of the angular velocity of body is:

$$\dot{\varphi}_i = K_G K_{Di}\dot{\beta} \tag{13}$$

Combining equations (5), (6), (7), (8), (9), (10), (11), (12) and (13) results in:

$$J_{eqi}\ddot{\beta} = \frac{K_G k_m K_{Di} U_i}{R_M} - \frac{k_E K_G^2 k_m K_{Di}^2 \dot{\beta}}{R_M} - \\ - b_{eqi}\dot{\beta} - M_{FRi}sign\left(\dot{\beta}\right) \tag{14}$$

In order to obtain an approximate solution for the non-linear equation, and taking into consideration that a filtering effect takes place in the mentioned system, the Krylov-Bogolubov method of equivalent linearization [6] is applied. For this purpose, a sinusoidal behavior of the expected solution is assumed:

$$\beta = aSin\left(\omega t\right), \tag{15}$$

where a is the amplitude, ω is the angular frequency, and t is the time. Next, near-identity transformations are introduced for the non-linear terms using the first-harmonics in the Fourier expansion. Nevertheless, before to present these transformations, it is important to remark that because of the complexity of the $K_{Di}(\beta)$ term, an additional approximation $\tilde{K}_{Di}(\beta)$ is required for it:

$$\tilde{K}_{D1}\left(\beta\right) = C_{A1} + C_{B1}\beta^2 \tag{16}$$

$$\tilde{K}_{D2}\left(\beta\right) = -C_{A2} - C_{B2}\beta^2 \tag{17}$$

These approximations are prepared taking into account that:

$$\min K_{D1}\left(\beta\right) \approx \min \tilde{K}_{D1}\left(\beta\right) \tag{18}$$

$$\max K_{D2}(\beta) \approx \max \tilde{K}_{D2}(\beta) \quad \text{and} \tag{19}$$

$$average\ K_{Di}(\beta) \approx average\ \tilde{K}_{Di}(\beta) \tag{20}$$

In this way, for the first regime:

$$\min \tilde{K}_{D1}(\beta) = 1 + \frac{L}{R} \qquad \text{and} \tag{21}$$

$$average\ \tilde{K}_{D1}(\beta) = 1 + \frac{\pi}{2\beta_0}, \tag{22}$$

and for the second regime:

$$|\max \tilde{K}_{D2}(\beta)| = -1 + \frac{L}{R} \qquad \text{and} \tag{23}$$

$$average\ \tilde{K}_{D2}(\beta) = \frac{\pi}{2\beta_0} - 1 \tag{24}$$

Then,

$$C_{A1} = 1 + \frac{L}{R} \tag{25}$$

$$C_{B1} = C_{B2} = \frac{3}{\beta_0^2}\left(\frac{\pi}{2\beta_0} - 1 - \frac{L}{R}\right) \tag{26}$$

$$C_{A2} = -1 + \frac{L}{R} \tag{27}$$

Once the approximation for the transmission ratio on each regime has been established, it is feasible to present the proposed near-identities transformations:

$$\tilde{K}_{Di}(\beta) U_i\left(\beta, \dot{\beta}\right) = \lambda_{0_i} + \lambda_{1_i}\beta + \lambda_{2_i}\dot{\beta} \tag{28}$$

$$\tilde{K}_{Di}^2(\beta)\dot{\beta} = \Delta_{0_i} + \Delta_{1_i}\beta + \Delta_{2_i}\dot{\beta} \tag{29}$$

$$M_{FRi} sign\left(\dot{\beta}\right) = \upsilon_{0_i} + \upsilon_{1_i}\beta + \upsilon_{2_i}\dot{\beta} \tag{30}$$

where $\lambda_{0_i}, \lambda_{1_i}, \lambda_{2_i}, \Delta_{0_i}, \Delta_{1_i}, \Delta_{2_i}, \upsilon_{0_i}, \upsilon_{1_i}$ and υ_{2_i} are coefficients of harmonic linearization. The calculation of these coefficients leads to:

$$\tilde{K}_{Di}(\beta) U_i\left(\beta, \dot{\beta}\right) = \frac{2(U_{Fi} - U_{0i})}{\pi}\left(\frac{C_{Ai}}{a} + \frac{2C_{Bi}a}{3}\right)\beta +$$

$$+\frac{2(U_{0i} + U_{Fi})}{\pi\omega_i}\left(\frac{C_{Ai}}{a} + \frac{C_{Bi}a}{3}\right)\dot{\beta} \tag{31}$$

$$\tilde{K}_{Di}^2(\beta)\dot{\beta} = \left[C_{Ai}^2 + \frac{1}{2}C_{Ai}C_{Bi}a^2 + \frac{1}{8}C_{Bi}^2 a^4\right]\dot{\beta} \tag{32}$$

$$M_{FRi} sign\left(\dot{\beta}\right) = \frac{4M_{FRi}}{\pi a\omega_i}\dot{\beta} \tag{33}$$

Due to the orthogonality of trigonometric functions, the next solution is obtained using the equations (14), (15), (16), (17), (25), (26), (27), (31), (32) and (33):

$$\begin{cases} J_{eqi}\omega_i^2 - \dfrac{2K_G k_m (U_{0i} - U_{Fi})}{\pi R_M}\left(\dfrac{C_{Ai}}{a} + \dfrac{2aC_{Bi}}{3}\right) = 0 \\ \dfrac{2K_G k_m (U_{0i} + U_{Fi})}{\pi\omega_i R_M}\left(\dfrac{C_{Ai}}{a} + \dfrac{aC_{Bi}}{3}\right) - b_{eqi} - \dfrac{4M_{FRi}}{\pi a\omega_i} - \\ \quad - \dfrac{k_E K_G^2 k_m}{R_M}\left(C_{Ai}^2 + \dfrac{1}{2}a^2 C_{Ai}C_{Bi} + \dfrac{1}{8}a^4 C_{Bi}^2\right) = 0 \end{cases}$$

On the other hand, considering that $\beta = aSin(\omega t)$ and $-\beta_0 < \beta < \beta_0$, it follows that

$$a = \beta_0 \tag{34}$$

In this point, if the constant voltage U_{0i} is defined, it is no trouble to search out the angular frequency ω_i:

$$\omega_i = \frac{-B_{\omega i} + \sqrt{B_{\omega i}^2 - 4A_{\omega i}C_{\omega i}}}{2A_{\omega i}}, \tag{35}$$

where:

$$A_{\omega i} = \frac{J_{eqi}\left(3C_{A_i} + a^2 C_{B_i}\right)}{\left(3C_{A_i} + 2a^2 C_{B_i}\right)}$$

$$B_{\omega i} = b_{eqi} + \frac{K_G^2 k_m k_E}{R_M}\left(C_{A_i}^2 + \frac{1}{2}a^2 C_{A_i}C_{B_i} + \frac{1}{8}a^4 C_{B_i}^2\right)$$

$$C_{\omega i} = \frac{4}{a\pi}\left[M_{FRi} - \frac{K_G k_m U_{oi}\left(3C_{A_i} + a^2 C_{B_i}\right)}{3R_M}\right]$$

Another option is to resolve several optimization problems for one specific regime or on the whole walking robot. For instance, on each regime is feasible to find the constant reduction gear ratio K_G value that minimizes the constant voltage U_0, while in a four-legged walking robot, it is possible to minimize the time of one walking cycle, or the power consumption.

IV. Control

An ideal tuning of the system takes place when the working element comes to the extreme position with a zero speed. It is also advisable to make this displacement in a minimal time, using all the possibilities that the electromotor and the transmission have available. However, the matter is that it is necessary to make this displacement when the information about some parameters (force of friction, random fluctuation, etc.) of the system is absent. One useful method to solve this issue is to apply a special algorithm of adaptive control elaborated earlier [7] for resonance drives as an adaptive control algorithm for the DUAL SMART drive. With this algorithm, the movement trajectory of each regime is divided into two equal parts - passive and active. On the passive part of the trajectory, the system operates under open loop control.

Feeding the drive motor with a constant voltage U_{0i} gives mobile parts the chance to move with a speed, which is defined by own properties of the system with a given configuration. In this way, the closest natural behavior of the system is achieved. During the process of movement, coordinate magnitudes are recorded into microprocessor's memory along with corresponding magnitudes of speed $(\varphi, \dot{\varphi})$. Once the mobile element has arrived to the middle position $\left(MP = \frac{\varphi_{final} - \varphi_{initial}}{2}\right)$, the active part of the trajectory starts. In this second part, a phase plane control is realized considering the pairs of data recorded previously, in such way that the trajectory is completed according to the symmetric law of movement (relative to the middle position). In other words, the algorithm makes a mirror of the stored pairs of data and uses this as tracking signal in phase plane control. More specifically, for each real system position, the symmetric velocity is calculated using a lineal extrapolation with the suitable data stored in the first passive part. With this reference velocity and the real velocity measured in the given position, the velocity error signal is determined. The process finishes when the system arrives to the final position with null velocity. Thus, the system behavior is perfectly symmetric and takes totally into account the intrinsic dynamic of the DUAL drive. Such algorithm is akin to conventional control algorithm with preliminary learning. However, unlike conventional approach, the learning does not take place before the working process but just during this working process, on the initial part of the trajectory. It has been shown that this algorithm can be used for DUAL SMART drive control in two regimes (movement of the crank within limits of angle γ_1 or γ_2) without operator intervention and without preliminary work in training regime.

The control algorithm is implemented directly in a 486 Processor running real time operating system QNX. QNX gives us the possibility to get both the number of clock cycles and the number of clock cycles' increments in one second for the processor, as a high performance mechanism for timing short intervals. Therefore, instead of measuring the velocity of the motor directly, it is calculated by using the position data and the real time from the operating system. Additionally, before using the velocity data, it is pre-processed, because some strategic points can be affected by noise. For this purpose each velocity measurement is passed through a low pass filter. The filter equation can be written in sequential mode as follow:

$$y_k = \left(\frac{a_2 - 1}{a_2 + 1}\right) y_{k-1} + k \left(\frac{1}{a_2 + 1}\right) (x_k + x_{k-1}) \qquad (36)$$

$$a_2 = \frac{2T_2}{Tm},$$

where y_k is the filtered velocity, y_{k-1} is the previous filtered velocity, x_k is the measured velocity, x_{k-1} is the previous measured velocity, T_2 is the dominant time constant in the system and T_m is the sampling period.

V. Experimental Results

To illustrate the use of the preceding concepts, a set of experiments was developed to estimate the performance of the system. For this purpose, a special prototype of the DUAL SMART drive was designed, manufactured and tested. Each experiment consisted of two parts. During the first part of the experiment, robot's leg was fixed on a base and a motion of robot's body was carried out. During the second part of the experiment, robot's body was fixed on the base and a movement of a robot's leg was performed. Figures 6 and 7 depict the motor behavior during the first and the second regimes respectively. It is relevant to mention that the angular velocity of the motor remains practically constant during the movement on each regime.

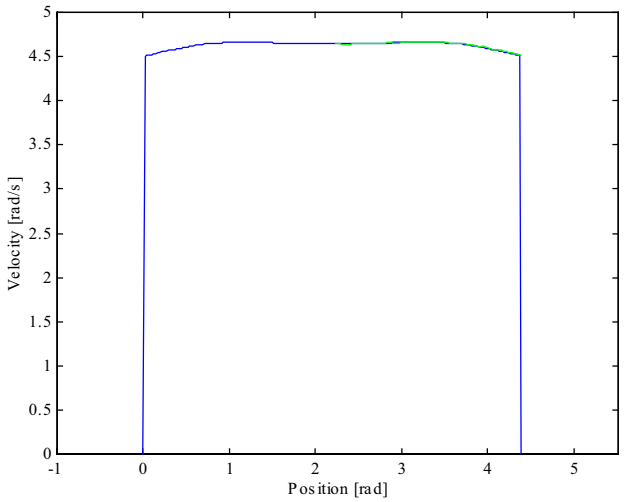

Fig. 6. Phase-plane of the motor in the first regime.

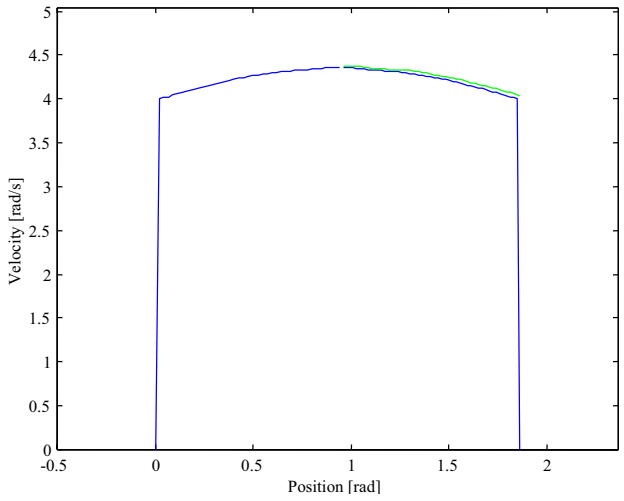

Fig. 7. Phase-plane of the motor in the second regime.

Figure 8 shows the experimentally obtained phase plane for the working element movement. The upper points

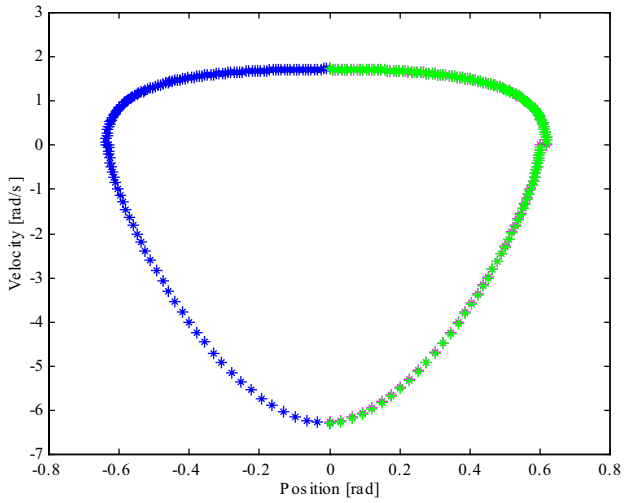

Fig. 8. Phase-plane of the mobile element.

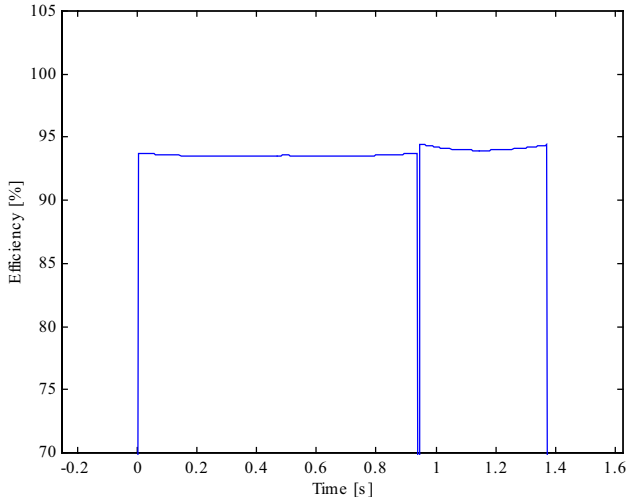

Fig. 9. Motor efficiency [%] vs. Time [s].

correspond to the robot's body movement (the crank displaces within the γ_1 angle limits), and the lower points correspond to the robot's leg movement (the crank displaces within the γ_2 angle limits). The upper and lower blue points correspond to the passive parts of the trajectories while the upper and lower green points correspond to the active parts of the trajectories. This phase plane obtained experimentally allows us to visually observe the motion pattern of the system.

Finally, figure 9 shows the high motor efficiency during both the first and the second regime.

VI. Conclusions

The effectiveness of usage of the DUAL SMART drive in those mechanisms, in which the same drive is used to perform two essentially different types of motions of the executive link, was confirmed. It was also shown that DUAL SMART, adjusted for realization of slow motion of a heavy robot body, could realize quick motion of the robot's leg. Through the analysis of the experimental results, the high motor efficiency in the start-stop movements was proved for each working regime. On the other hand, the adaptive control algorithm was used successfully for the DUAL SMART drive. This algorithm maintains a reliable work of the drive while different constructive parameters of it are changing, without operator intervention and without a preliminary learning. Consequently, future work in this area will address the test of the DUAL SMART drive in a real walking robot.

Acknowledgments

The authors would like to acknowledge the financial support from Ministry of Science and Technology of Spain (Project "Theory of optimal dual drives for automation and robotics") and from Ministry of Culture and Education of Spain (Fellowship F.P.U.).

References

[1] Akinfiev T., Armada M. *Resonance and quasi-resonance drives for start-stop regime*, Proceedings of the 6th International Conference MECHATRONICS'98, Skovde, Sweden. Pergamon, pp. 91-96, 1998.

[2] Akinfiev T., Armada M., Fontaine J.-G. *The way of increasing effectiveness of machines operating in start-stop regime*, IFAC Workshop on European Scientific and Industrial Collaboration on promoting "Advanced Technologies in Manufacturing" WESIC'98, June 10-12, 1998, Girona, Spain, Proceedings, pp. 421-424.

[3] Van De Straete H., De Schutter J. *Optimal time varying transmission for servo motor drives*, Proceedings of the Tenth World Congress on the Theory of Machines and Mechanisms. IFToMM, Oulu University Press, ISBN 951-42-5287-X, Vol. 5, 1999, pp. 2055-2062.

[4] Caballero R., Akinfiev T., Montes H., and Armada M. *On the modelling of SMART non-linear actuator for walking robots*, Proceedings of the Fourth International Conference on Climbing and Walking Robot. Edited by Karsten Berns and Rüdiger Dillman. Professional Engineering Publishing limited, London, UK, 2001, pp. 159-166. ISBN 1-86058-365-2.

[5] Akinfiev, T., Fernández, R., Armada, M. *Dual Smart Drive for walking robots*, Proceedings of the Fifth International Conference on Climbing and Walking Robots and their supporting Technologies. Edited by Philippe Bidaud and Faiz Ben Amar. Professional Engineering Publishing Limited. London, UK, 2002, pp. 595-602. ISBN: 1-86058-380-6.

[6] Besekerskii V., Popov E. *Theory of Automatic Control Systems*, Nauka, Moscow, Russia, 1975.

[7] Akinfiev T. *Method of controlling of mechanical resonance hand*, Patent USA 4958113.